Experimental Lung Research

ISSN: 0190-2148 (Print) 1521-0499 (Online) Journal homepage: https://www.tandfonline.com/loi/ielu20

QUANTITATIVE IMAGE ANALYSIS OF LUNG CONNECTIVE TISSUE IN MURINE SILICOSIS

James M. Antonini, David R. Hemenway & Gerald S. Davis

To cite this article: James M. Antonini, David R. Hemenway & Gerald S. Davis (2000) QUANTITATIVE IMAGE ANALYSIS OF LUNG CONNECTIVE TISSUE IN MURINE SILICOSIS, Experimental Lung Research, 26:2, 71-88, DOI: 10.1080/019021400269880

To link to this article: https://doi.org/10.1080/019021400269880

Published online: 02 Jul 2009.

Experimental Lung Research, 26: 71–88, 2000

0190-2148/00 $12.00 + .00

QUANTITATIVE IMAGE ANALYSIS OF LUNG CONNECTIVE TISSUE IN MURINE SILICOSIS

James M. Antonini □ *Health Effects Laboratory Division, National Institute for Occupational Safety and Health, Morgantown, West Virginia, USA*

David R. Hemenway □ *Department of Civil and Mechanical Engineering, University of Vermont, Burlington, Vermont, USA*

Gerald S. Davis □ *Department of Medicine, University of Vermont, Burlington, Vermont, USA*

□ *Pulmonary fibrosis is a disabling consequence of many lung diseases but is difficult to quantify. Lucifer yellow CH fluorescent dye (LY) appears to stain connective tissue matrix macromolecules selectively. Laser scanning confocal microscopy can quantify the intensity of fluorescence and determine the area of fluorescent material. We hypothesized that the abundance of lucifer yellow–stained matrix macromolecules in lung tissue sections could be measured by laser scanning confocal microscopy, would reflect differences between varying degrees of pulmonary fibrosis, and could be compared directly to biochemical measurements of lung collagen. We exposed C57B1/6 and 129 strains of mice by aerosol to cristobalite silica (70 mg/m^3, 12 days, 5 hours/day) or sham-air and examined them 2 and 16 weeks after exposure. The area of LY-stained matrix in tissue sections was quantitated by laser scanning confocal microscopy, and total lung collagen was measured biochemically as hydroxyproline (OH-proline). The LY-stained connective tissue matrix appeared as bright linear bands in the alveolar septae, and was increased significantly by image analysis in C57B1/6 and 129 mice with silicosis 16 weeks after exposure. Total lung OH-proline was significantly increased in silica-exposed mice from both stains at both time points. Comparing all 8 groups, there was a significant linear correlation between the average area of connective tissue measured by LY stain and the total OH-proline per lung measured by chemical analysis* ($r = .72$, $P = .042$). *LY staining and confocal microscopy with image analysis offers a rapid technique for quantitative measurements of the extent of pulmonary fibrosis.*

Keywords *collagen, image analysis, laser scanning confocal microscopy, lung, mouse, inbred strains, pulmonary fibrosis, silica, silicosis*

Received 11 November 1998; accepted 29 June 1999.

This work was supported by grant RO1-HL47069 from the National Heart, Lung, and Blood Institute. Dr. Antonini is supported by funding from the National Institute for Occupational Safety and Health, Morgantown.

The authors thank Linda M. Pfeiffer, Michael C. Miller, and Tina G. Charron for their technical assistance; Lyndell Millecchia, PhD, for her help in the preparation of the manuscript; and Charles G. Irvin, PhD, for his constructive suggestions for this report.

Address correspondence to Gerald S. Davis, MD, Director, Pulmonary Disease and Critical Care Medicine, Given C-317, College of Medicine, University of Vermont, Burlington, VT 05405, USA. E-mail: gdavis1@zoo.uvm.edu

Pulmonary fibrosis may accompany chronic occupational lung diseases such as silicosis or asbestosis, chronic diseases of unknown etiology such as idiopathic pulmonary fibrosis, chronic collagen-vascular diseases such as progressive systemic sclerosis (scleroderma), chronic infection as in cystic fibrosis, and as the consequence of acute lung injury as in the acute respiratory distress syndrome (ARDS). The presence of excess connective matrix at inappropriate anatomic sites in the lung may be readily apparent as a qualitative change in histologic tissue sections, but it is difficult to measure this change quantitatively. Total lung collagen can be measured biochemically [1], but this approach requires fresh tissue, destroys the specimen by digestion, and is best applied to a defined anatomic lung unit for expression of the results.

Lucifer yellow CH fluorescent dye appears to stain connective tissue matrix macromolecules selectively [2], permitting optical visualization of matrix material when a histology section is illuminated with ultraviolet light. Laser scanning confocal microscopy provides a method to quantify the intensity of fluorescence, and to determine the total area of fluorescent material with defined levels of intensity within a specified area of examination. The overall goal for the present research was to employ lucifer yellow stain and confocal microscopy to quantitate the extent of pulmonary fibrosis in lung tissue sections. We pursed this goal by examining tissues from a well-characterized animal model of pulmonary fibrosis, silicosis in the mouse [3–13].

Silicosis is a chronic diffuse parenchymal lung disease that results from exposure for prolonged periods to airborne respirable dust containing crystalline silica particles. In addition to its importance as an occupational lung disease, silicosis may serve as an example in which to study pulmonary fibrosis. We reported recently on the features of silicosis in mice exposed by inhalation to an aerosol of cristobalite silica [13]. These animals developed diffuse pulmonary pathological changes consistent with silicosis in rodents, demonstrated an expanded air-space population of cells enriched for macrophages, lymphocytes, and neutrophils, and showed increased lung hydroxyproline content as a reflection of increased lung collagen. At an early time point following silica exposure (2 weeks), the lung tissues appeared normal or showed slight accumulation of neutrophils and macrophages in the alveolar spaces, but increased connective tissue matrix or widening of the alveolar septae were not apparent. At a later time point after exposure (16–20 weeks), the mice showed the pathology of silicosis in rodents: focal parenchymal lesions, interstitial thickening with more apparent connective tissue matrix, and air spaces filled with cells and exudate. At 16 to 20 weeks after silica inhalation, lung collagen was increased to 155% of parallel air-sham control levels in the silica-exposed mice.

Laser scanning confocal microscopy offers many advantages over conventional microscopic techniques. The shallow depth of field of confocal micro-

scopes allows information to be collected from a well-defined optical section, rather than thicker superimposed structures within the specimen as in the conventional light microscope [14]. Consequently, out-of-focus light is virtually eliminated, which results in an increase in contrast, clarity, and detection sensitivity [15]. The confocal microscope optically sections specimens so that some of the physical sectioning artifacts observed with conventional light and electron microscopy are eliminated. The basic image analysis and display systems integrated with the commercially available laser scanning confocal microscopes provide ease of operation, rapid image formation, and digital image collection for morphometric analysis [16, 17]. The excitation and detection wavelengths available with the scanning laser and video camera extend the range that could be achieved with conventional optical fluorescence light microscopes.

Lucifer yellow has been used in a previous study to visualize large volumes of lung parenchyma with imaging by laser scanning confocal microscopy [18]. Rogers and colleagues [2] demonstrated that elastin, collagen, and other components of lungs treated with lucifer yellow were readily distinguished and measured, and could be reconstructed three-dimensionally. In a preliminary report, Antonini and associates used lucifer yellow stain and laser scanning confocal microscopy to quantitate pulmonary fibrosis without physical destruction of the tissue specimens from rats treated with intratracheal silica instillation [19].

We hypothesized that the abundance of lucifer yellow–stained matrix macromolecules in lung tissue sections could be measured by laser scanning confocal microscopy, that the automated image measurements would reflect differences between varying degrees of pulmonary fibrosis, and could be compared directly to biochemical measurements of lung collagen. We tested this hypothesis in mice exposed by aerosol inhalation to cristobalite silica using 2 strains of mice, groups exposed to sham-air or silica, and early and late time points, in order to provide animals with varying amounts of lung connective tissue macromolecules.

METHODS

Inhalation Exposure Conditions

Mice (*Mus musculus*) of the strains C57B1/6 and 129 were purchased at 6 weeks of age from the Jackson Laboratory (Bar Harbor, ME). Mice were kept in filter top cages held in laminar flow housing racks, and were provided with food and water ad libitum. The mice were exposed after 1 to 2 weeks of observation in our facility. Aerosol exposure to silica was carried out utilizing a horizontal flow inhalation toxicology system that has been described in detail [13, 20–22]. The mice were exposed to an aerosol of cristobalite silica

(C & E Minerals, King of Prussia, PA) generated with a modified Wright dust feed apparatus. The mice were divided into air-sham control or silica-exposed groups, and were exposed to the HEPA filtered, humidified, temperature-controlled carrier air stream or to the mineral dust in identical chambers for 5 hours per day for a total of 12 days at an average ambient dust concentration of 69.5 ± 10.6 mg/m^3.

Tissue Histology Specimens

Tissues were prepared for histopathology and for analysis of total lung collagen 2 weeks and 16 weeks after the silica aerosol exposure was completed. Mice were killed by intraperitoneal injection of an overdose of sodium pentobarbital (0.7 mg/mouse), the trachea cannulated, the thorax opened, and the lungs reinflated by gentle injection of 4% phosphate-buffered formalin fixative through the airway catheter until they reached approximately normal anatomic volume, and the airway pressure was held for 3 to 5 minutes at 10 cm H_2O pressure above the level of the right atrium as measured with a water column manometer. Cubes of lung tissue were removed after fixation in situ, gently agitated in the fixative at room temperature for 24 hours, and then washed and stored in 70% ethanol fixative. Tissue was embedded in paraffin and sectioned for staining with haematoxylon and eosin (H & E) or with lucifer yellow (LY) dye.

Confocal Microscopy and Image Analysis

Slides with thin sections of lung tissue were treated with lucifer yellow CH (Molecular Probes, Eugene, OR; 0.1 mg/mL in 100% ethanol) for 24 hours. After incubation, the slides were rinsed with 100% ethanol, and coverslips were applied. Images were recorded using a Sarastro 2000 (Molecular Dynamics, Inc., Sunnyvale, CA) laser scanning confocal microscope (Optiphot-2, Nikon, Inc., Melville, PA) fitted with an argon ion laser. Emission spectra >510 nm were diverted to a separate photodetector and used to image lung tissue and cells.

Using a $20\times$ objective, we randomly scanned 25 regions of lung parenchyma from each of the lung samples. Large airways and blood vessels were excluded. An image field 1024 μm $\times$ 1024 μm (1.05×10^6 μm^2) was defined over a region of parenchyma entirely filling the field. With the ImageSpace software (Molecular Dynamics), we established threshold pixel intensity levels that defined lucifer yellow–positive and lucifer yellow–negative sites, and thus identified the presumed connective tissue matrix material. Fluorescent signals below a pixel intensity value of 16 were thresholded out, which eliminated the measurement of cells and debris within the air spaces. We determined the tissue area above the pixel intensity threshold

for each of the images generated. All random scans of the lung tissue for each treatment group were recorded at a photo multiplier tube (PMT) setting range of 480 to 520. This analysis resulted in a data set expressed as connective tissue (lucifer yellow–positive) area in μm^2 per image field, with 25 measurements for each of 2 mice from each strain, time point, and treatment group. For statistical analysis of differences between groups, the 25 measurements from 2 mice were merged into a single data set of 50 values per group.

Lung Collagen

Total lung collagen was inferred by measuring the hydroxyproline (OH-proline) content of the entire right and left lung parenchyma from 3 mice at each time and exposure condition using modifications of the methods of Prockop and colleagues [1] and Woessner [23], as previously reported [13]. The data were expressed as μg OH-proline per lung.

Statistical Analyses

Values for lucifer yellow confocal microscopy area of connective tissue or for total lung OH-proline from air-sham control and silica-exposed groups of mice were compared using Student's *t* test for nonpaired samples, and by analysis of variance (ANOVA) with Scheffe post hoc evaluation for the data set as a whole. The area of lung connective tissue measured by confocal microscopy image analysis and the total OH-proline content of the lung were correlated for groups of mice of each strain, exposure condition, and time point using linear regression analysis. The statistical analyses were performed using a statistical package for MS-DOS microcomputers (Systat 7.01 for Windows, SPSS, Inc., Chicago, IL).

RESULTS

Silicosis in C57Bl/6 and 129 Strain Mice

Mice of both the C57Bl/6 and the 129 strains evidenced normal behavior and no overt physical signs of respiratory distress following silica exposure. Body weight gain was comparable between air-sham and silica-exposed mice within each strain. Lung tissues appeared normal and identical in air-sham control animals from both strains. In control tissue, the alveolar septae were delicate and the air spaces were empty except for scattered macrophages (Figure 1*a*). Bronchus-associated lymphoid tissue (BALT) aggregates could be found occasionally at airway bifurcations.

Both C57Bl/6 and 129 mice developed experimental silicosis following inhalation exposure to cristobalite silica. The microscopic appearance of the lung parenchyma was similar to that reported previously for C3H/HeN mice

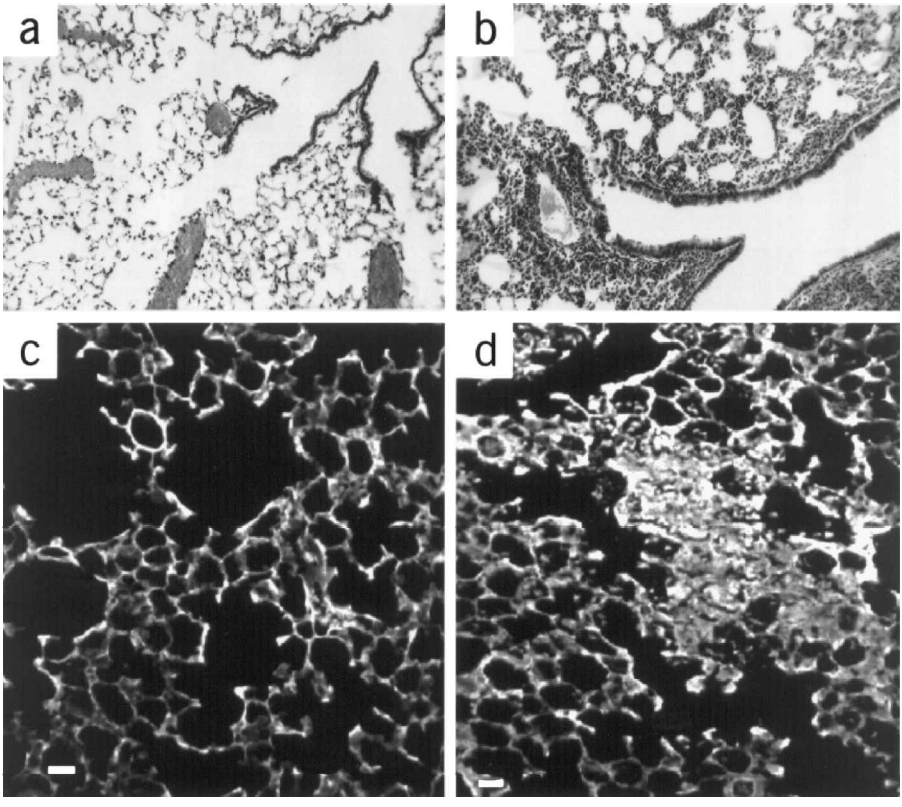

FIGURE 1 Silicosis in C57Bl/6 and 129 strain mice. Representative lung tissue sections from air-sham control and cristobalite silica-exposed mice (70 mg/m^3, 12 days, 5 hours/day) from the C57Bl/6 and 129 strains and mice 16 weeks after exposure are shown. The appearance of the C57B1/6 and 129 mice for each exposure condition were not distinguishable from each other. (*a*) Air-sham control, C57Bl/6 strain. Normal mouse lung parenchyma is illustrated by delicate alveolar septae and empty air spaces, as seen by visual light microscopy. Occasional large free alveolar cells, probably macrophages, can be seen. H & E stain, original magnification 100×. (*b*) Silica-exposed, 129 strain. Silicosis in the mouse is evidenced by focal lesions consisting of macrophages, lymphocytes, fibroblasts, interstitial thickening, proteinaceous exudate, and small bands of connective tissue matrix material. H & E stain, original magnification 100×. (*c*) Air-sham control, C57B1/6 strain. Viewed by laser scanning confocal microscopy, bright linear lucifer yellow fluorescent staining is evident in short segments of the alveolar septate in the normal lung parenchyma. The length bar indicates 20 μm. Lucifer yellow stain, original magnification 100×. (*d*) Silica-exposed, C57Bl/6 strain. Extensive lucifer yellow fluorescent staining is evident in the alveolar septae and within organizing lesions in a silicotic mouse lung. Inflammatory exudate and other cell material appears as gray autofluorescence, whereas empty air spaces appear black. The length bar indicates 20 μm. Lucifer yellow stain, original magnification 100×.

[13]. Two weeks after exposure the lung tissues demonstrated a slight increase in the apparent number of air-space macrophages and neutrophils, and occasional small cell aggregates. Changes in the width or complexity of the alveolar septae were not evident by qualitative visual examination at this early time point. Sixteen weeks after silica exposure substantial pathological changes were notable in lung tissue from both strains, as illustrated in Figure

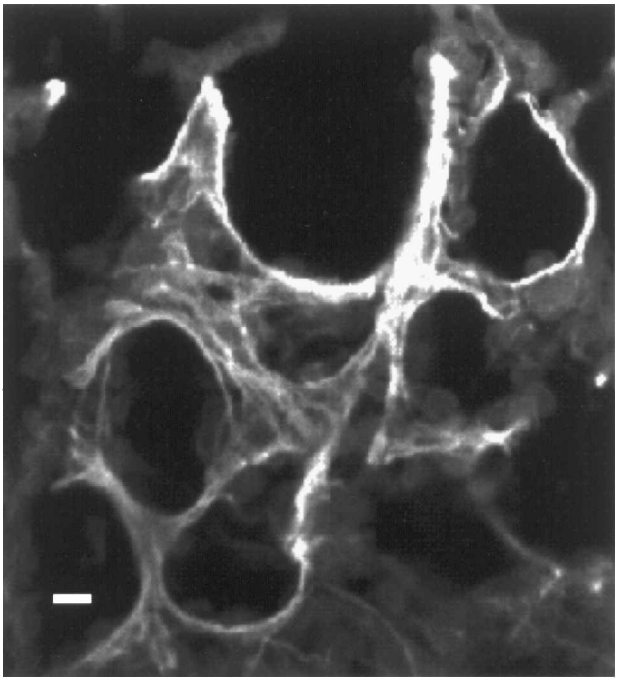

FIGURE 2 Connective tissue matrix in silicosis. A high-magnification image from confocal laser scanning microscopy of lucifer yellow–stained lung tissue from a silicotic mouse reveals dense linear bands of connective tissue matrix material within the alveolar walls. The length bar indicates 10 μm. C57B1/6 mouse, 16 weeks post–silica inhalation, lucifer yellow stain.

1*b*. Focal lesions consisting of macrophages, lymphocytes, fibroblasts, interstitial thickening, proteinaceous exudate, and small bands of connective tissue matrix material were seen throughout the lung parenchyma on H & E–stained sections. BALT structures were more numerous and appeared enlarged compared with the air-sham control lungs. Lymphocytic infiltrates were evident within the lung parenchyma. Thickening and distortion of alveolar septae were apparent as a qualitative changes at the later time point.

Bronchoalveolar lavage specimens from C57Bl/6 and 129 strain mice showed results similar to those reported previously for other strains exposed to silica under similar conditions [13], with recruitment of neutrophils evident at 2 weeks and a substantial increase in the numbers of macrophages, lymphocytes, and neutrophils observed at 16 weeks (data not shown).

Image Analysis of Lung Connective Tissue

Qualitative examination of LY-stained lung sections revealed connective tissue elements using laser scanning confocal microscopy. A bright linear fluorescent signal was evident in short segments of the alveolar septae in the normal lung parenchyma from the air-sham control mice (Figure 1*c*). More

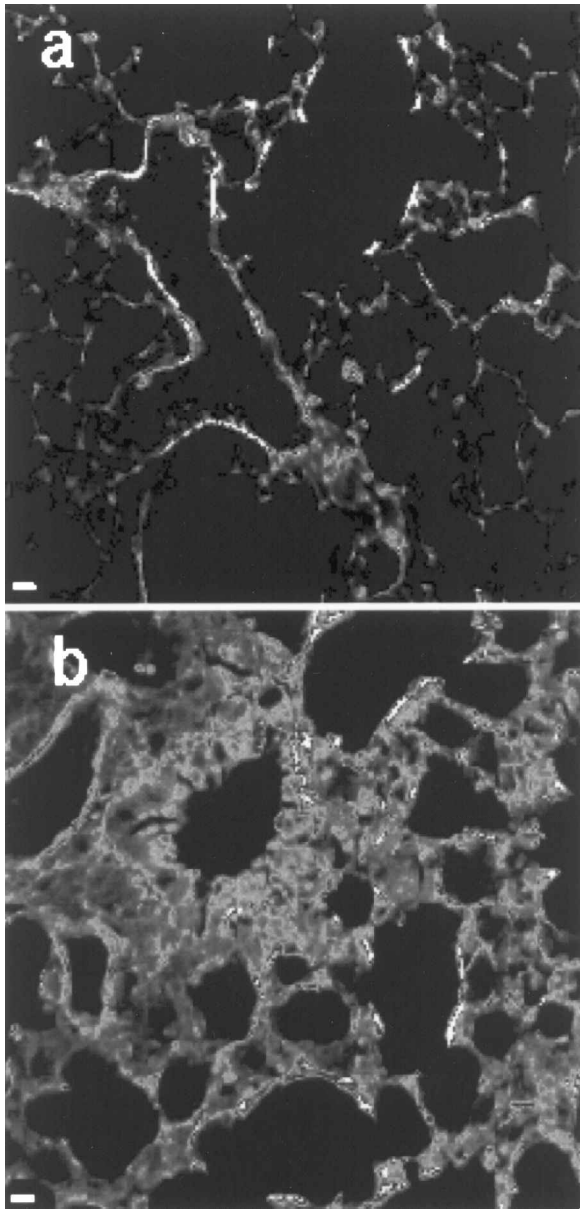

FIGURE 3 Image analysis by confocal microscopy. Mouse lung tissue sections stained with lucifer yellow fluorescent dye were examined by laser scanning confocal microscopy, and the intensity of fluorescence was measured at each pixel. The pixel intensity was divided into 6-scale cohorts, and each cohort was assigned a color. Background areas appear purple (empty air spaces), low intensity sites appear blue (tissue autofluorescence), and increasingly high intensity areas (connective tissue matrix) appear as green, yellow, red, or white. (*a*) Air-sham control mouse lung. A normal lung demonstrates small lines of connective matrix in alveolar septae. The length bar indicates 20 μm. C57B1/6 mouse 16 weeks after exposure to sham air; lucifer yellow stain, original magnification 100×. (*b*) Silica-exposed mouse lung. A lung with silicosis reveals diffuse thickening of the alveolar walls with extensive bright regions of fluorescent matrix material. The length bar indicates 20 μm. C57B1/6 mouse, 16 weeks after silica inhalation; lucifer yellow stain, original magnification 100×.

extensive fluorescent staining was evident in the alveolar septae and within the organizing lesions of the silicotic mouse lungs (Figure 1*d*). Inflammatory cells and cellular exudate appeared gray, whereas empty air spaces were black. An increase in the abundance of LY-stained connective tissue was observed over time with the development of silicosis, paralleling the findings in the conventional H & E–stained sections (Figure 1*b*). At higher magnifications, thick abundant bands of lung connective tissue were observed easily within the alveolar walls of specimens from the silicotic mice, as shown in Figure 2.

For quantitation of pulmonary fibrosis, lung sections were examined by laser scanning confocal microscopy and the intensity of LY fluorescence at each pixel was measured. The brightness intensity was ranked into 6 categories, and a display color assigned to each category by the image analysis computer program. Figure 3 shows color images of air-sham and silicotic mouse lung specimens displayed in this manner. The number of pixels within the image area demonstrating brightness intensity above a defined threshold were considered positive for LY staining, and were summed to calculate the total connective tissue area in μm^2 per image area. Background areas were displayed in purple (empty air spaces), low intensity sites appeared blue (tissue autofluorescence), and increasingly high intensity areas (connective tissue matrix) were displayed as green, yellow, red, or white. The normal lung sections demonstrated small bright lines of connective tissue in the alveolar septae (Figure 3*a*). Lung sections from silica-exposed mice revealed diffuse thickening of the alveolar walls with extensive bright regions of fluorescent matrix material (Figure 3*b*).

The results of quantitative image analysis of LY-stained lung tissue sections are shown in Figure 4. Two mice were examined from each strain, exposure condition, and time point group. Due to an accident, only 1 animal was available for the 129 strain air-sham group at 2 weeks after exposure. The individual animal mean values from 25 image area measurements are shown as error bars, and the average for the 2 mice as the hatched bar height. In air-sham control mouse lungs 2 weeks postexposure, the area of LY-stained connective matrix in the lung parenchyma of both strains averaged 103, 710 μm^2 per image area, or 9.9% of the image area. Silica inhalation did not result in a significant increase in the LY-stained area 2 weeks after the exposure. At 16 weeks after exposure, the mice in both strains that had inhaled silica demonstrated a substantial increase in the area of LY-stained connective tissue. The increase associated with silicosis at 16 weeks was significant, both in comparison to the air-sham mice at 16 weeks ($P < .001$) and in comparison with the air-sham or silica-exposed mice at 2 weeks ($P < .001$). The extent of connective tissue staining and the increases related to silicosis were similar in the C57Bl/6 (Figure 4*a*) and the 129 (Figure 4*b*) strains.

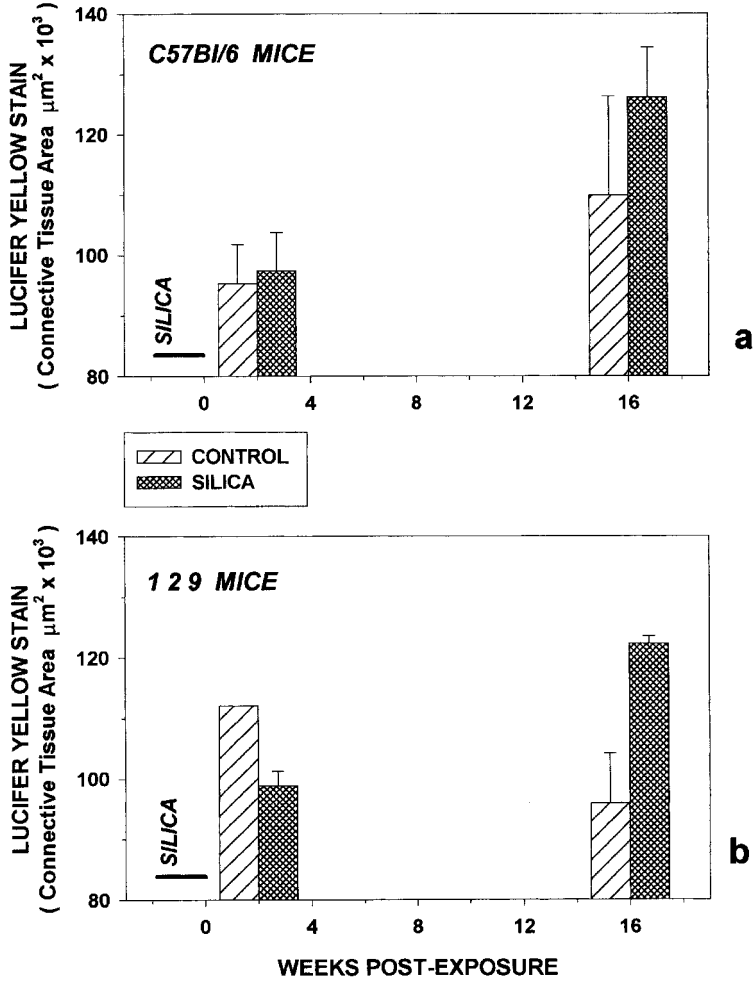

FIGURE 4 Connective tissue area by image analysis. The area of connective tissue stained positively by lucifer yellow dye was quantitated by laser scanning confocal microscopy as fluorescence above a threshold level, and expressed as the connective tissue area in μm^2 per image area (ordinate). A total of 25 image areas over lung parenchyma were examined to express the mean area for each mouse. For each strain, exposure condition, and time point, the minimum and maximum mouse values are shown as error bars, and the average for two mice per group as the height of the hatched bar. For statistical testing by analysis of variance with Scheffe post hoc evaluation, the 50 area measurements for one group were compared with the 50 measurements from each of the other groups. The period of exposure (12 days, 5 hours/day) to cristobalite silica (70 mg/m^3) or sham air is shown as a horizontal bar, with subsequent time after exposure shown in weeks (abscissa). (*a*) C57Bl/6 strain mice. At 2 weeks postexposure, air-sham and silica-exposed mice were similar with regards to the area of connective tissue matrix. At 16 weeks there was a significant increase in the connective tissue area in the silica-exposed mice compared to the air-sham mice ($P < .001$) and also compared to either group at 2 weeks ($P < .001$). The area was also greater for the air-exposed mice at 16 weeks compared to 2 weeks ($P < .002$). (*b*) 129 strain mice. The 129 strain mice exposed to silica showed a significant increase in lung connective tissue area compared to the air sham controls 16 weeks after exposure ($P < .001$). Only 1 mouse was available for analysis in the air-sham group 2 weeks after exposure.

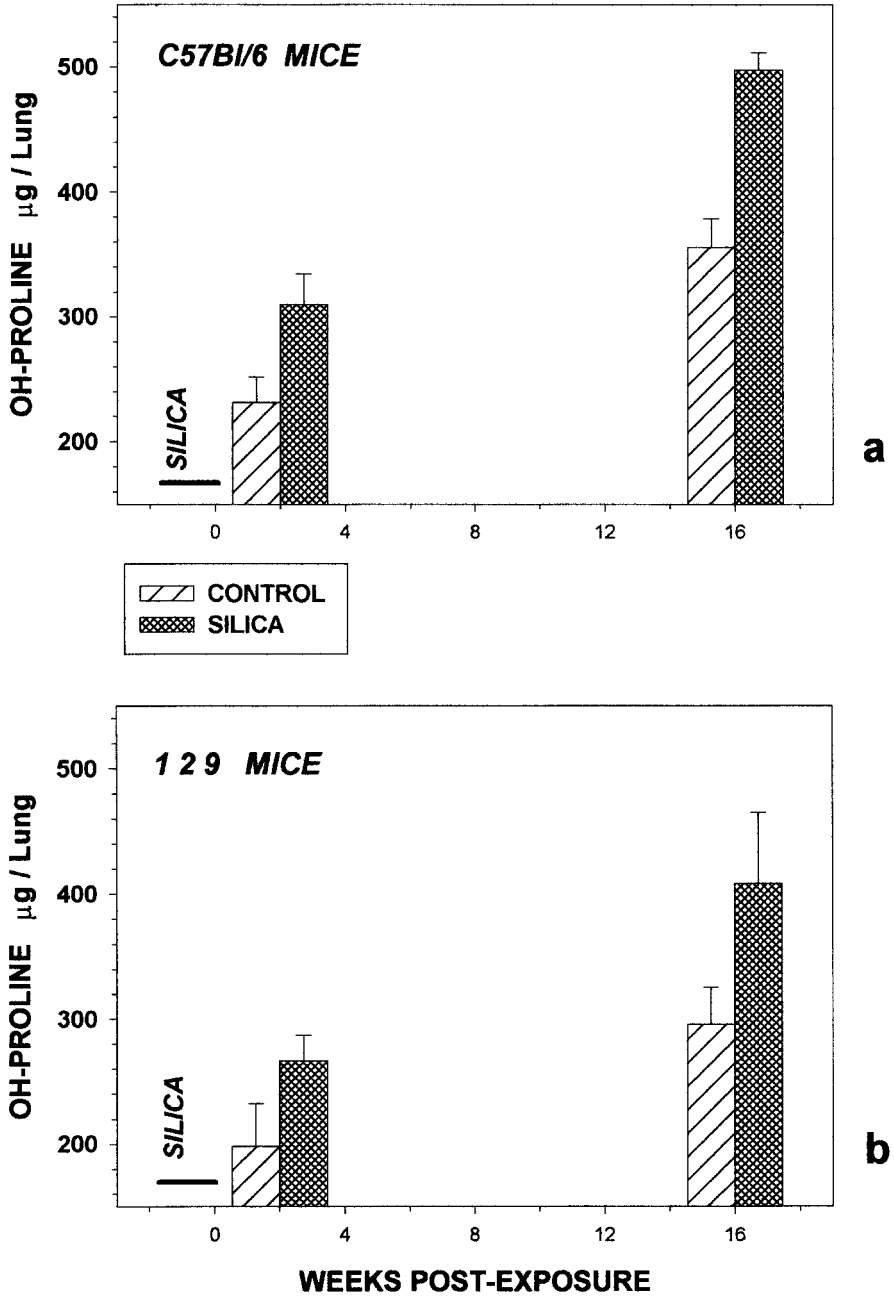

FIGURE 5 Total lung collagen. The collagen in each mouse lung was estimated by quantitation of OH-proline. The whole lungs from 3 mice in each group were analyzed, and the results expressed as the mean ± *SEM*, shown in the same format as Figure 4. The total collagen in the lungs of mice exposed to silica was increased significantly ($P < .04$) at both 2 weeks and 16 weeks postexposure in both the C57B1/6 strain mice (*a*) and the 129 strain mice (*b*). In both strains the total lung collagen at 16 weeks was significantly greater than at 2 weeks in both the air-sham ($P < .03$) and silica-exposed ($P < .04$) groups.

Total Lung Collagen

The measurements of total lung collagen (tested as OH-proline) are shown in Figure 5*a* for the C57Bl/6 and 5b for the 129 mice. In both strains the amount of lung collagen in control air-sham mice increased significantly between 2 weeks and 16 weeks ($P < .03$), reflecting body growth. Silica exposure caused a significant increase in total lung collagen in both strains and at both time points ($P = .04$ or less for all comparisons).

Comparison of Connective Analysis Techniques

A relationship was observed between the amount of total lung collagen (OH-proline) from biochemical analysis and the area of LY-stained lung connective tissue from image analysis. This relationship is shown for all strains, time points, and exposure conditions in Figure 6. The line of best fit by least-squares regression is shown as well. The average area of connective tissue staining measured by image analysis correlated significantly with the average biochemical measurement of OH-proline for each group of mice ($r = .72$,

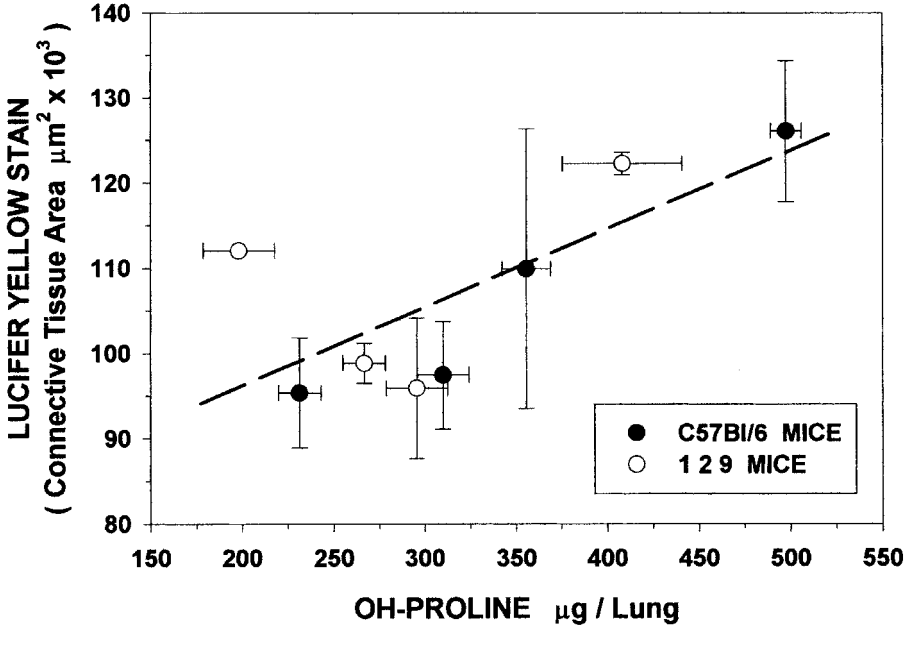

FIGURE 6 Comparison of image analysis and biochemical techniques. The mean values for lung connective tissue area by lucifer yellow staining with laser scanning confocal microscopy image analysis are plotted against the total lung OH-proline for C57B1/6 mice (closed circles) and 129 strain mice (open circles) by exposure condition and time after inhalation exposure. Error bars represent individual values for image analysis area (2 mice per group) and *SEM* values for OH-proline (3 mice per group). The dashed line represents the linear regression line of best fit for all 8 data points, a significant relationship ($r = .72$, $P = .042$).

$P < .05$). Only one air-sham control mouse was available at 2 weeks from the 129 strain for image analysis, and this single data point deviated somewhat from the regression line. Most groups fit the relationship well, with the greatest or the smallest values for both LY-stained area and OH-proline measurement occurring in the same group.

DISCUSSION

Silicosis in C57B1/6 and 129 Mouse Strains

The features of silicosis in C57Bl/6 and 129 strain mice were very similar to those we have reported previously for C3H/HeN mice [13]. Examination of H & E–stained tissue sections from both strains used for this report showed few abnormalities 2 weeks after cristobalite silica exposure was completed, and extensive abnormalities 16 weeks after exposure. The lack of tissue change immediately after dust exposure suggests that the disease process in this model system is not merely a response to acute lung injury, but rather is a chronic response to the presence of silica in the lung. In this regard the model resembles accelerated or chronic silicosis in man [24]. We utilized this model system to provide lung tissue specimens with normal or abnormal histology, and with a range of values for both image analysis and biochemical measurements of connective tissue matrix.

Qualitative examination of LY-stained tissue sections demonstrated that connective tissue matrix elements could be found with this technique in the normal (air-sham control) lung (Figure 1*c*). The location, appearance, and abundance of stained connective tissue changed with evolving silicosis (Figure 1*d*), paralleling the appearance of silicotic lesions and widened alveolar septae in conventional H & E–stained sections (Figure 1*b*). The quantitative image analysis measurements of the area of LY-stained matrix in various lung sections provided a range of average values from 95×10^3 to 126×10^3 μm^2 per image field for comparison with features of strain and exposure, and for correlation with biochemical measurements. The analysis of total lung collagen measured biochemically as OH-proline provided a range of values from 198 to 498 μg per lung for these comparisons.

LY image analysis and biochemical OH-proline measurements both demonstrated statistically significant differences based on strain, exposure to silica, and time after exposure as presented above (Figures 4 and 5). For each group of mice, there was a significant direct correlation between the amount of OH-proline measured biochemically, and the area of LY staining assessed by image analysis (Figure 6). These results demonstrate that LY staining with quantitative image analysis can detect differences in the extent of pulmonary fibrosis in mice with silicosis, and that measurements obtained by this method parallel results of qualitative visual examination and biochemical quantization.

The two approaches, LY stain with image analysis and biochemical determination of OH-proline, may measure somewhat different constituents in the lung. The LY dye appears to become associated with dense, fibillar collagen, thus this stain may detect mainly mature, crosslinked, type I collagen. The extent of binding to other collagen types, to nascent less crosslinked type I collagen, or to elastin and other matrix elements, is not known. The biochemical technique measures the abundance of hydroxylated proline in acid-digested tissues, and may detect many types of collagen as well as elastin. Raghu and colleagues [25] described the location and abundance of various collagen isotypes in lung tissue sections from patients with idiopathic pulmonary fibrosis (IPF), demonstrating a large increase in type I collagen but also increased abundance of type III collagen. Type I collagen characterized late fibrosis with extensive disease, whereas type III collagen was more abundant in early interstitial lung disease. Coxson and associates [25A] used electron microscopy and morphometry to study human lung specimens, and showed a large increase in fibrillar collagen with little or no increased elastin in IPF patients.

These observations may help to explain the differences we observed between LY-stained tissue sections and biochemical measurements of OH-proline. At the early time point, 2 weeks after exposure, biochemical total lung collagen was significantly increased in both C57B1/6 and 129 mice exposed to silica, whereas LY-stained sections showed no increases in connective tissue matrix area compared to the air-sham controls. This disparity could reflect biochemical detection of type III collagen, nascent type I collagen, and other early response elements that did not avidly bind LY dye. At the later time point, 16 weeks after silica exposure, significant increases in both the microscopic and the biochemical measurements were seen in both strains among the silica-exposed mice. We postulate that at this time point there was abundant mature type I collagen that was detected by both methods.

There are limitations imposed by the technical requirements for each of these two methods. The biochemical approach can be performed in most laboratories, but it is somewhat laborious, and in mice requires all of one lung or both lungs for accurate analysis. The biochemical measurement of lung collagen is most accurate if an anatomic unit (e.g., whole lung or lobe) is used as the denominator to express the results. Because lung weight usually increases with inflammation, edema, and fibrosis, expression of lung OH-proline per weight unit may underestimate the degree of collagen accumulation that has occurred [26]. The LY image analysis approach can be performed on small amounts of tissue or on previously embedded tissue samples. The degree of inflation of the tissue during fixation might influence the area of connective tissue matrix relative to the area of the image, because less inflated lung would contain more tissue and less air space than well-

inflated specimens. This should not be a limitation in animal studies (such as ours) in which all specimens can be handled identically and inflated to a standard physiologic pressure. Variation in the degree of inflation might be a problem in human lung biopsy specimens where standardization is difficult to achieve. The LY stain can be performed easily, and can be examined qualitatively with widely available UV light fluorescence microscopy equipment. Lung tissue autofluorescence may be problematic at these excitation and visualization wavelengths. Image analysis may be difficult due autofluorescence and to the somewhat blurred image sometimes seen. Confocal microscopy with quantitative image analysis requires expensive and specialized equipment that may not be available to some researchers. If available, confocal laser scanning microscopy offers sharp imaging through optical sectioning, avoidance of much autofluorescence through advantageous excitation and detection wavelengths, and automated image analysis capabilities.

Measurements of Fibrosis in Tissue Sections

Investigators over the past decade have utilized semiquantitative grading schemes, morphometry, and computer-based image analysis to assess the extent of abnormalities in human idiopathic pulmonary fibrosis (IPF). Initial efforts described simple scales [27–29], or linear point intercept morphometry [30] to assess the extent of fibrosis, inflammation, and tissue abnormality. A detailed system of semiquantitative scoring utilizing light microscopic examination of lung biopsy specimens by multiple pathologists showed good correlation among the various components of the scoring system [31] and moderate inter- and intraobserver variation [32], but poor correlation with pulmonary function testing [33]. Semiquantitative scales of disease extent and severity in lung biopsies of IPF patients have shown reasonable correlation with features identified radio graphically by high-resolution computed tomography (HRCT) scanning [34, 35].

Lung morphometry utilizes histology section images to count the interceptions between tissue components of interest and a superimposed grid of lines or dots [36, 37]. Well-validated statistical methods can then be employed to calculate the area density or the number of each component in the section. If the lungs have been prepared appropriately, the volume density or absolute number of each component in the whole lung can be estimated. These approaches can be applied to conventional sections examined by light microscopy, but are often used with transmission electron microscopy in order to identify individual cell types with confidence. Evaluation by morphometry provides detailed numerical information, but it is very labor intensive. Morphometry was used to enumerate myofibroblasts and other cell types in the lungs of rats with bleomycin-induced pulmonary fibrosis [38]. Morphometric analysis of the extent of fibrosis in the lungs

of bleomycin-treated rabbits showed good correlation with biochemical measurements of total lung collagen (OH-proline) [39].

Computer-based image analysis has been used to express the extent of abnormality in a tissue section as a percentage of the area of interest, producing data similar to that presented in this report. Image analysis was used to relate the thickness of arterial walls in lung tissue sections with the stage of disease for coal workers with pneumoconiosis [40]. Assessing the extent of fibrosis in human liver biopsies stained for collagen with Sirius red F3BA dye, a semiquantitative grading system correlated moderately well with computer-based image analysis of the fractional area of fibrosis [41]. Image analysis was used to assess the extent of fibrosis in radiation-induced pulmonary fibrosis in the mouse, examining tissues stained with Sirius red and imaged electronically [42], or stained with H & E and delineating fibrosis with the margins drawn manually [43].

These reports indicate that in human IPF a semiquantitative grading scale of tissue abnormalities offers limited accuracy and reproducibility, and fair or moderate correlation with radiographic HRCT, physiologic, or global clinical assessment of the extent of disease. Tissue morphometry is often not possible or practical for human lung biopsy specimens because complete anatomic lung units are not removed, fixation at true anatomic volume is difficult, and morphometry requires a large investment of time for tissue examination. In animal model systems where all parameters can be controlled more closely, both morphometry and image analysis appear to provide accurate measures of tissue events, and reasonable correlations with other biochemical or radiographic measurements of the extent of fibrosis. Image analysis might offer a compromise between the limitations encountered with human pathological specimens and the accuracy of automated information processing.

Future Applications

LY fluorescent dye staining and laser scanning confocal microscopy with image analysis offers a rapid and apparently accurate technique for quantitative measurements of the extent of pulmonary fibrosis in lung tissue sections. This approach may be useful for research applications where pathological tissue is already available, or when large amounts of tissue cannot be allocated for biochemical analysis. The microscopic technique may allow localization of connective tissue accumulation to specific anatomic compartments (e.g., alveolar parenchyma, bronchial wall, subpleural, etc.), whereas biochemical measurements cannot. Image analysis may be applicable to human lung biopsy specimens where biochemical analysis is not feasible, and where an anatomic unit cannot be used as the denominator for expressing the results. Future studies should test the sensitivity and utility of

LY staining with quantitative image analysis of lung connective tissue in other animal models of lung disease and in biopsy specimens from human patients with pulmonary fibrosis.

REFERENCES

1. Prockop DJ, Udenfriend S: A specific method for the analysis of hydroxyproline in tissues and urine. Anal Biochem. 1960;1:228–239.
2. Rogers RA, Oldmixon EH, Brain JD: Enhanced contrast within embedded tissue by lucifer yellow CH: an ideal stain for laser scanning confocal microscopy. Mol Biol Cell. 1992;3:185a.
3. King EJ, Mohanty GP, Harrison CV, Nagelschmidt G: The action of different forms of pure silica on the lungs of rats. Br J Industr Med. 1953;10:9–17.
4. Heppleston AG, Stiles JA: Activity of a macrophage factor in collagen formation by silica. Nature. 1967;214:521–522.
5. Harrington JS, Ritchie M, King PC, Miller K: The in-vitro effects of silica-treated hamster macrophages on collagen production by hamster fibroblasts. J Pathol. 1973;109:21–37.
6. Last JA, Reiser KM: Effects of silica on lung collagen. Ciba Found Symp. 1986;121:180–193.
7. Ramos C, Montano M, Gonzalez G, Vadillo F, Selman M: Collagen metabolism in experimental lung silicosis. A trimodal behavior of collagenolysis. Lung. 1988;166:347–353.
8. Wiessner JH, Mandel NS, Sohnle PG, Hasegawa A, Mandel GS: The effect of chemical modification of quartz surfaces on particulate-induced pulmonary inflammation and fibrosis in the mouse. Am Rev Resp Dis. 1990;141:111–116.
9. Benson SC, Belton JC, Scheve LG: Regulation of lung fibroblast proliferation and protein synthesis by bronchiolar lavage in experimental silicosis. Environ Res. 1986;41:61–78.
10. Callis AH, Sohnle PG, Mandel GS, Wiessner J, Mandel NS: Kinetics of inflammatory and fibrotic pulmonary changes in a murine model of silicosis. J Lab Clin Med. 1985;105:547–553.
11. Li YR, Hu X, Yang BZ: Studies on structural changes of collagen in silicosis. Biomed Environ Sci. 1994;7:302–306.
12. Mariani TJ, Roby JD, Mecham RP, Parks WC, Crouch E, Pierce RA: Localization of type I procollagen gene expression in silica-induced granulomatous lung disease and implication of transforming growth factor-beta as a mediator of fibrosis. Am J Pathol. 1996;148:151–164.
13. Davis GS, Leslie KO, Hemenway DR: Silicosis in mice: effects of dose, time, and genetic strain. J Environ Pathol Toxicol Oncol. 1998;17:81–97.
14. Wright SJ, Centonze VE, Stricker SA, DeVries PJ, Shatten G: Introduction to confocal microscopy and three-dimensional reconstruction. In: Matsumoto B, ed. Methods in Cell Biology. New York, NY: Academic Press; 1993:1–45.
15. Shotten DM: Confocal scanning optical microscopy and its applications for biological specimens. J Cell Sci. 1989;94:175–206.
16. Pawley J: The Handbook of Biological Confocal Microscopy. Madison, WI: IMR Press; 1989.
17. Smith GJ, Bagnell CR, Bakewell WE, et al: Application of confocal scanning laser microscopy in experimental pathology. J Electr Microsc. 1991;18:38–49.
18. Oldmixon EH, Carlsson K: Methods for large data volumes from confocal scanning laser microscopy of lung. J Microsc. 1993;170:221–228.
19. Antonini JM, Charron TG, Lai J, Blake TL, Rogers RA: The introduction of laser scanning confocal microscopy for the analysis of particle-induced lung fibrosis. Am J Respir Crit Care Med. 1998;157:149a.
20. Hemenway DR, MacAskill SM: Design, development and test results of a horizontal flow inhalation toxicology facility. Am Ind Hyg Assoc J. 1982;43:874–879.
21. Hemenway DR, Absher MP, Trombley L, Vacek PM: Comparative clearance of quartz and cristobalite from the lung. Am Ind Hyg Assoc J. 1990;51:363–369.
22. Hemenway DR, Sylvester D, Gale PN, Vacek P, Evans JN: Effectiveness of animal rotation in achieving uniform dust exposure and lung dust deposition in horizontal flow chambers. Am Ind Hyg Assoc J. 1983;44:655–658.
23. Woessner JF: The determination of hydroxyproline in tissue and protein samples containing small proportions of this imino acid. Arch Biochem Biophys. 1961;93:440–447.

24. Davis GS: Silica. In: Harber P, Schenker MB, Balmes JR, eds. Occupational and Environmental Respiratory Disease. St. Louis, MO: Mosby–Year Book; 1996;373–399.
25. Raghu G, Striker LJ, Hudson LD, Striker GE: Extracellular matrix in normal and fibrotic human lungs. Am Rev Respir Dis. 1985;131:281–289.
25A. Coxson HO, Hogg JC, Mayo JR, Behzad H, Whittall KP, Schwartz DA, Hartley PG, Galvin JR, Wilson JS, Hunninghake GW: Quantification of idiopathic pulmonary fibrosis using computed tomography and histology. Am J Resp Crit Care Med. 1997;155:1649–1656.
26. Fulmer JD, Bienkowski RS, Cowan MJ, et al: Collagen concentration and rates of synthesis in idiopathic pulmonary fibrosis. Am Rev Respir Dis. 1980, 122:289–301.
27. Watters LC, King TE, Schwarz MI, Waldron JA, Stanford RE, Cherniack RM: A clinical, radiographic, and physiologic scoring system for the longitudinal assessment of patients with idiopathic pulmonary fibrosis. Am Rev Respir Dis. 1986;133:97–103.
28. Ashcroft T, Simpson JM, Timbrell V: Simple method of estimating severity of pulmonary fibrosis on a numerical scale. J Clin Pathol. 1988;41:467–470.
29. Harrison NK, Myers AR, Corrin B, et al: Structural features of interstitial lung disease in systemic sclerosis. Am Rev Respir Dis. 1991;144:706–713.
30. Gil J, Marchevsky AM, Jeanty H: Septal thickness in human lungs assessed by computerized interactive morphometry. Lab Invest. 1988;58:466–472.
31. Hyde DM, King TEJ, McDermott T, et al: Idiopathic pulmonary fibrosis. Quantitative assessment of lung pathology. Comparison of a semiquantitative and a morphometric histopathologic scoring system. Am Rev Respir Dis. 1992;146:1042–1047.
32. Cherniack RM, Colby TV, Flint A, et al: Quantitative assessment of lung pathology in idiopathic pulmonary fibrosis. The BAL Cooperative Group Steering Committee. Am Rev Respir Dis. 1991;144:892–900.
33. Cherniack RM, Colby TV, Flint A, et al: Correlation of structure and function in idiopathic pulmonary fibrosis. Am J Respir Crit Care Med. 1995;151:1180–1188.
34. Muller NL, Staples CA, Miller RR, Vedal S, Thurlbeck WM, Ostrow DN: Disease activity in idiopathic pulmonary fibrosis: CT and pathologic correlation. Radiology. 1987;165:731–734.
35. Kazerooni EA, Martinez FJ, Flint A, et al: Thin-section CT obtained at 10-mm increments versus limited three-level thin-section CT for idiopathic pulmonary fibrosis: correlation with pathologic scoring. AJR Am J Roentgenol. 1997;169:977–983.
36. Cassan SM, Divertie MB, Brown ALJ: Fine structural morphometry on biopsy specimens of human lung. 2. Diffuse idiopathic pulmonary fibrosis. Chest. 1974;65:275–278.
37. Bolender RP, Hyde DM, Dehoff RT: Lung morphometry: a new generation of tools and experiments for organ, tissue, cell, and molecular biology. Am J Physiol. 1993;265:L521–L548.
38. Adler KB, Callahan LM, Evans JN: Cellular alterations in the alveolar wall in bleomycin-induced pulmonary fibrosis in rats. An ultrastructural morphometric study. Am Rev Respir Dis. 1986;133:1043–1048.
39. Hirose N, Lynch DA, Cherniack RM, Doherty DE: Correlation between high resolution computed tomography and tissue morphometry of the lung in bleomycin-induced pulmonary fibrosis in the rabbit. Am Rev Respir Dis. 1993;147:730–738.
40. Wang H, Li J: Quantitative morphological studies on pulmonary arteriole in coal workers (in Chinese). Chung Hua Yu Fang I Hsueh Tsa Chih. 1996;30:209–212.
41. Chevallier M, Guerret S, Chossegros P, Gerard F, Grimaud JA: A histological semiquantitative scoring system for evaluation of hepatic fibrosis in needle liver biopsy specimens: comparison with morphometric studies. Hepatology. 1994;20:349–355.
42. Kraus R, Steinberg F, Rehn B, Bruch J, Streffer C: Radiation-induced changes in lung tissue and development of fibrosis determined by quantitative morphometric methods. J Cancer Res Clin Oncol. 1991;117:27–32.
43. Haston CK, Travis EL: Murine susceptibility to radiation-induced pulmonary fibrosis is influenced by a genetic factor implicated in susceptibility to bleomycin-induced pulmonary fibrosis. Cancer Res. 1997;57:5286–5291.